ARTHRITIS & RHEUMATISM
Vol. 60, No. 5, May 2009, pp 1390–1405
DOI 10.1002/art.24443

Cartilage Repair in a Rat Model of Osteoarthritis Through Intraarticular Transplantation of Muscle-Derived Stem Cells Expressing Bone Morphogenetic Protein 4 and Soluble Flt-1

Tomoyuki Matsumoto,[1] Gregory M. Cooper,[1] Burhan Gharaibeh,[1] Laura B. Meszaros,[1] Guangheng Li,[2] Arvydas Usas,[2] Freddie H. Fu,[3] and Johnny Huard[1]

Objective. **The control of angiogenesis during chondrogenic differentiation is an important issue affecting the use of stem cells in cartilage repair, especially with regard to the persistence of regenerated cartilage. This study was undertaken to investigate the effect of vascular endothelial growth factor (VEGF) stimulation and the blocking of VEGF with its antagonist, soluble Flt-1 (sFlt-1), on the chondrogenesis of skeletal muscle-derived stem cells (MDSCs) in a rat model of osteoarthritis (OA).**

Methods. **We investigated the effect of VEGF on cartilage repair in an immunodeficiency rat model of OA after intraarticular injection of murine MDSCs expressing bone morphogenetic protein 4 (BMP-4) in combination with MDSCs expressing VEGF or sFlt-1.**

Results. **In vivo, a combination of sFlt-1– and BMP-4–transduced MDSCs demonstrated better repair without osteophyte formation macroscopically and histologically following OA induction, when compared with the other groups. Higher differentiation/proliferation and lower levels of chondrocyte apoptosis were also observed in sFlt-1– and BMP-4–transduced MDSCs compared with a combination of VEGF- and BMP-4–transduced MDSCs or with BMP-4–transduced MDSCs alone. In vitro experiments with mixed pellet coculture of MDSCs and OA chondrocytes revealed that BMP-4–transduced MDSCs produced the largest pellets, which had the highest gene expression of not only type II collagen and SOX9 but also type X collagen, suggesting formation of hypertrophic chondrocytes.**

Conclusion. **Our results demonstrate that MDSC-based therapy involving sFlt-1 and BMP-4 repairs articular cartilage in OA mainly by having a beneficial effect on chondrogenesis by the donor and host cells as well as by preventing angiogenesis, which eventually prevents cartilage resorption, resulting in persistent cartilage regeneration and repair.**

Osteoarthritis (OA), a chronic degenerative joint disorder with worldwide impact, is characterized by articular cartilage destruction and osteophyte formation. OA affects >40 million individuals in the US alone and influences more lives than any other musculoskeletal condition (1). Since articular cartilage is a tissue type that is poorly supplied by blood vessels, nerves, and the lymphatic system, it has a very limited capacity for repair after injury. Although several therapies have been used for OA, no widely accepted treatments have been established, with the exception of arthroplasty. For this reason, tissue engineering techniques aimed at repairing articular cartilage have been extensively studied, and chondrocyte transplantation has already been performed (2–4).

Currently, the most effective treatment for OA, besides arthroplasty, is autologous chondrocyte transplantation. However, this treatment has several limitations, including the need to use neighboring healthy

Supported by the US Department of Defense (contract (W81XWH-08-0076). Dr. Huard's work was supported by the William F. and Jean W. Donaldson Chair at the Children's Hospital of Pittsburgh, and the Henry J. Mankin Endowed Chair for Orthopaedic Research at the University of Pittsburgh.

[1]Tomoyuki Matsumoto, MD, PhD, Gregory M. Cooper, PhD, Burhan Gharaibeh, PhD, Laura B. Meszaros, BS, Johnny Huard, PhD: Children's Hospital of Pittsburgh, and University of Pittsburgh, Pittsburgh, Pennsylvania; [2]Guangheng Li, MD, PhD, Arvydas Usas, MD: Children's Hospital of Pittsburgh, Pittsburgh, Pennsylvania; [3]Freddie H. Fu, MD: University of Pittsburgh, Pittsburgh, Pennsylvania.

Dr. Huard has received consulting fees from Cook Myosite, Inc. (more than $10,000) and receives royalties from Cook Myosite, Inc. for the licensing through the University of Pittsburgh of patented technology for the preplate technique for isolation of muscle-derived stem cells.

Address correspondence and reprint requests to Johnny Huard, PhD, Stem Cell Research Center, Children's Hospital of Pittsburgh, 4100 Rangos Research Center, 3705 Fifth Avenue, Pittsburgh, PA 15213-2582. E-mail: jhuard@pitt.edu.

Submitted for publication September 3, 2008; accepted in revised form January 19, 2009.

donor cartilage, difficulty in treating large-scale defects, limited expansion capacity of primary chondrocytes, and the need for a periosteal patch to maintain engineered cartilage. In addition, in most cases only 30–40% of the defect regenerates articular cartilage, with the remaining defect being filled with fibrocartilage (5,6).

In light of these limitations, it is important to find other sources of cells that are abundant and capable of chondrogenic differentiation. Muscle stem cells are more attractive than primary chondrocytes because of their superior capacity for self-renewal, proliferation, and survival following environmental stress (7–9). Recently, stem cell–based therapies have been used clinically for cartilage repair (10,11). The results of several previous studies, including those using muscle-derived stem cells (MDSCs), have indicated that stem cells can undergo chondrogenesis and repair articular cartilage in experimental cartilage injury models (12–15). We previously demonstrated that bone morphogenetic protein 4 (BMP-4)–transduced MDSCs improved cartilage formation in an in vitro pellet culture and regeneration in an in vivo cartilage defect model (13). Based on those results, the present study was designed to clarify the therapeutic efficacy of BMP-4–transduced MDSCs in OA.

The control of angiogenesis during chondrogenic differentiation is one of the most important issues affecting the application of stem cells for cartilage repair. Among angiogenesis-modulating factors, including antiangiogenic factors such as troponin 1 (16) and chondromodulin 1 (17), vascular endothelial growth factor (VEGF) is an important mediator of angiogenesis (18). VEGF stimulates capillary formation in vivo and exerts direct mitogenic actions on various cells in vitro (19). In the growth plate, VEGF has been reported to play an essential role in cartilage vascularization and absorption of hypertrophic chondrocytes, which together lead to ossification (20,21). Similar to this endochondral ossification, osteophyte formation during OA development has been reported to involve VEGF signaling (22).

Similarly, recent data reveal the expression of VEGF and its receptors (Flt-1 and Flk-1) in OA cartilage and reflect the ability of VEGF to enhance catabolic pathways in chondrocytes by stimulating matrix metalloproteinase (MMP) activity and reducing tissue inhibitors of MMPs (TIMPs) (23–25). These data suggest that, apart from the effect of VEGF on cartilage vascularization and proliferation of cells in the synovial membrane, chondrocyte-derived VEGF promotes catabolic pathways in the cartilage itself, thereby leading to a progressive breakdown of the extracellular matrix (ECM) of articular cartilage.

In the current study, we used a gain- and loss-of-function approach based on tissue engineering techniques to assess the role of VEGF in MDSC-mediated cartilage repair. We demonstrated that genetically modified MDSCs expressing a VEGF antagonist and BMP-4 and transplanted intracapsularly in a rat model of OA enhanced chondrogenesis, repaired cartilage via the autocrine/paracrine effects of BMP-4, and contributed to an appropriate environment that prevented chondrocyte apoptosis by blocking both the intrinsic VEGF catabolic pathway and extrinsic VEGF-induced vascular invasion. This is the first report to describe the effects of VEGF on MDSC-mediated chondrogenesis and OA repair in vitro and in vivo.

MATERIALS AND METHODS

Isolation of MDSCs. MDSCs were isolated from the hind limb skeletal muscle of 3-week-old male C57BL/10J mice (The Jackson Laboratory, Bar Harbor, ME) via a previously described modified preplate technique (7).

Retroviral transduction. Retroviral vectors encoding for green fluorescent protein (GFP), BMP-4 and GFP (BMP-4–GFP), human $VEGF_{165}$ and bacterial nuclear-localized LacZ (VEGF-LacZ), or human soluble Flt-1 (sFlt-1), a VEGF antagonist, and LacZ (sFlt-1–LacZ) expression were generated as previously described (26). Transduction efficiency was ~80% for each retroviral vector. MDSCs were transduced separately with these retroviral vectors at a multiplicity of infection of 5 in the presence of 8 μg/ml of Polybrene. The transduced cells were expanded for 2 weeks before being used in experiments, and the conditioned media were sampled to determine transgene expression. The level of BMP-4 secreted from the transduced cells was estimated with a BMP-4 bioassay, as previously described (27). The levels of VEGF or sFlt-1 secreted by the transduced cells were confirmed by enzyme-linked immunosorbent assay (ELISA) as previously described (28).

Repair of mono-iodoacetate (MIA)–induced arthritis. The animal experiments conducted as a part of this study were approved by the Animal Research and Care Committee at Children's Hospital of Pittsburgh. Sixty 10-week-old female nude rats (NIH-*Whn* NIHRNU-M; Taconic, Germantown, NY) were used. The animals were anesthetized with 3% isoflurane and O_2 gas (1.5 liters/minute) delivered through an inhalation mask. OA-like arthritis was induced by a single intraarticular injection of MIA (Aldrich Chemical, Milwaukee, WI) (0.3 mg per 150 mg body weight) into both knee joints of the rats.

Rats were divided into 2 groups based on OA model (n = 30 rats [60 knees] per group) and further divided into 5 groups based on treatment type (n = 6 rats [12 knees] per group). The 2 models of OA were a chronic disease model in which rats were intraarticularly injected with cells after OA had progressed significantly (2 weeks after MIA injection) and a subacute disease model in which rats were treated with cells before significant OA progression (1 week after MIA injection). Rats in treatment group 1 received 2.5×10^5 sFlt-1–transduced MDSCs combined with 2.5×10^5 BMP-4–transduced MDSCs in phosphate buffered saline (PBS) (sFlt-

1/BMP-4–MDSC group). Group 2 rats were treated with 2.5×10^5 VEGF-transduced MDSCs combined with 2.5×10^5 BMP-4–transduced MDSCs in PBS (VEGF/BMP-4–MDSC group). Group 3 rats were treated with 5.0×10^5 BMP-4–transduced MDSCs in PBS (BMP-4–MDSC group). Group 4 rats were treated with 5×10^5 MDSCs in PBS (MDSC group), and group 5 rats were treated with PBS alone (PBS group). Rats were allowed to move freely within their cages after cell injection. Rats were killed 4 weeks (both chronic OA and subacute OA models), 12 weeks (chronic OA model), or 16 weeks (subacute OA model) after cell transplantation (n = 6 OA knees for each time point).

Tissue harvest. After macroscopic examination, 6 distal femora per group per time point were dissected for histologic and histochemical staining and fixed with 10% neutral buffered formalin for 48 hours, followed by decalcification with 10% EDTA for 2 weeks and paraffin embedding. For immunohistochemical staining, 6 distal femora per group at week 4 were harvested and quickly embedded in OCT compound (Miles, Elkhart, IN), snap-frozen in liquid nitrogen, and stored at −80°C until used.

Histologic evaluation of cartilage repair. Sagittal sections (5 μm thick) were obtained and stained with Safranin O–fast green. We evaluated OA repair semiquantitatively using a grading and staging system (29). This system included 6 histologic grades and 4 histologic stages. The total score (grade multiplied by stage) ranged from 1 point (normal articular cartilage) to 24 points (no repair).

Contribution of transduced MDSCs to cartilage healing. Rat femurs in OCT-embedded blocks were sectioned, and 5-μm serial sections were mounted on silane-coated glass slides and air dried for 1 hour before being fixed with 4.0% paraformaldehyde at 4°C for 5 minutes and stained immediately. To detect transplanted mouse cells in the articular cartilage of the femoral condyle, immunohistochemistry was performed at week 4 (in 6 additional rats in each group) with the following antibodies: rabbit anti–rat type II collagen (Col2) (Sigma, St. Louis, MO) to detect rat and mouse chondrocytes (mouse via cross-reactivity of the antibody with mouse Col2 [13]), Alexa Fluor 488–conjugated rabbit anti-GFP (Molecular Probes, Eugene, OR) for detection of BMP-4 and GFP–transduced MDSCs and GFP-transduced MDSCs, and biotin-conjugated anti–β-galactosidase (anti–β-gal) for detection of sFlt-1 and LacZ–transduced MDSCs and VEGF and LacZ–transduced MDSCs.

GFP or LacZ genes were used to distinguish the contributions of BMP-4–transduced MDSCs from those of nontransduced MDSCs and of sFlt-1–transduced MDSCs from those of VEGF-transduced MDSCs. In addition, due to green autofluorescence in GFP, red fluorescence was applied for LacZ staining to avoid false-positive staining. Double immunohistochemistry with GFP or β-gal and Col2 was performed to detect the contribution of transduced MDSCs to cartilage healing. To assess the contribution of intracapsular-injected MDSCs, the number of double-positive or Col2-positive cells was morphometrically counted as the average value in 5 randomly selected articular cartilage areas in the femoral condyle. The following secondary antibodies were used for each immunostaining: Cy3-conjugated or fluorescein isothiocyanate (FITC)–conjugated anti-rabbit antibody (Molecular Probes) for Col2 staining, and Cy3-conjugated streptavidin (Molecular Probes) for β-gal staining. For nuclear staining, 4′,6-diamidino-2-phenylindole (DAPI) solution was applied for 5 minutes.

Analysis of chondrocyte apoptosis and proliferation. Sagittal paraffin-embedded sections (5 μm thick) were obtained, and the TUNEL assay was performed at week 4 using an Apop Tag Plus Peroxidase In Situ Apoptosis Detection kit according to the recommendations of the manufacturer (Chemicon, Temecula, CA). Briefly, sections were incubated with 15 μg/ml of proteinase K for 15 minutes at room temperature, and then washed in PBS. Endogenous peroxidase was quenched with 3% H_2O_2 for 5 minutes at room temperature. After washing in PBS, sections were immersed in buffer containing terminal deoxynucleotidyl transferase enzyme and incubated for 90 minutes at 37°C in a humid atmosphere. After washing again in PBS, sections were incubated with antidigoxigenin conjugate for 30 minutes at room temperature. After washing in PBS and developing color in peroxidase substrate with diaminobenzidine, signals were examined by microscopy (n = 6 rats from each treatment group).

To measure cell proliferation, immunohistochemistry was performed, using additional animals at week 4, on formalin-fixed, bromodeoxyuridine (BrdU)–incorporated, paraffin-embedded sections, as previously described (20). BrdU was administered intraperitoneally to rats, at 50 mg/kg, 1 and 24 hours before the rats were killed in order to incorporate enough BrdU. After a 20-minute treatment with 0.05% trypsin at 37°C and a 45-minute treatment with 95% formamide in 0.15*M* trisodium citrate at 70°C for denaturing, tissues were stained overnight at 4°C with mouse biotin-conjugated anti-BrdU (Zymed, San Diego, CA) at a dilution of 1:1,000. Signals were then detected using the Vectastain ABC Standard Elite kit (Vector, Burlingame, CA) (n = 6 rats from each treatment group). Labeled nuclei were counted in 5 independent, randomly selected fields.

Isolation of rat OA chondrocytes and normal mouse chondrocytes. Articular cartilage was removed from the femoral condyles of rats 2 weeks after injection of MIA under sterile conditions. The tissue fragments were cut into 1-mm slices and washed 4 times with PBS containing 100 units/ml of penicillin and 100 μg/ml of streptomycin. Slices were cut into small pieces and incubated for 16–24 hours with 1.5 mg/ml of collagenase B (Roche, Mannheim, Germany) and 1 m*M* cysteine in Dulbecco's modified Eagle's medium (DMEM). The cell suspension was filtered through a 20-μm nylon mesh to remove debris and washed 3 times with calcium-free DMEM. The cells were seeded at a density of 100,000 cells/cm^2 overnight at 37°C in a humidified atmosphere containing 5% CO_2 and used for each experiment. Similarly, normal mouse chondrocytes were isolated from mouse articular cartilage and used as controls.

Mixed pellet culture. Pellet culture was performed as described previously (30). Mixed pellet cultures consisted of the following: 1) 0.5×10^5 sFlt-1–transduced MDSCs, 0.5×10^5 BMP-4–transduced MDSCs, and 1.0×10^5 OA chondrocytes (sFlt-1/BMP-4–MDSC plus chondrocytes group), 2) 0.5×10^5 VEGF-transduced MDSCs, 0.5×10^5 BMP-4–transduced MDSCs, and 1.0×10^5 OA chondrocytes (VEGF/BMP-4–MDSC plus chondrocytes group), 3) 1.0×10^5 BMP-4–transduced MDSCs and 1.0×10^5 OA chondrocytes (BMP-4–MDSC plus chondrocytes group), 4) 1.0×10^5 nontransduced MDSCs and 1.0×10^5 OA chondrocytes (MDSC plus chondrocytes group), and 5) 2.0×10^5 OA chondrocytes

(chondrocytes group). Pellets were made in 0.5 ml of chondrogenic medium that contained DMEM supplemented with 1% penicillin/streptomycin, $10^{-7}M$ dexamethasone, 50 μg/ml of ascorbate 2-phosphate, 40 μg/ml of proline, 100 μg/ml of pyruvate, and 1% BD ITS+ (insulin–transferrin–selenium) premix (Becton Dickinson, Franklin Lakes, NJ) with 10 ng/ml of transforming growth factor β3 (R&D Systems, Minneapolis, MN). The pellets were incubated at 37°C in 5% CO_2, and the medium was changed every 2 to 3 days. Pellets were harvested after 14 days in culture.

Separated pellet culture. MDSCs and OA chondrocytes were separated by sterilized culture plate insert (Millicell; Millipore, Bedford, MA). Pellets of OA chondrocytes were made in the medium at the bottom of a 15-ml tube, as previously described (31). The membrane plate was inserted into the 15-ml tube so that the MDSC pellets were placed within the membrane plate. Separated pellets were made with 1) 1.0×10^5 sFlt-1–transduced MDSCs, 1.0×10^5 BMP-4–transduced MDSCs, and 2.0×10^5 OA chondrocytes (sFlt-1/BMP-4–MDSC plus chondrocytes group), 2) 1.0×10^5 VEGF-transduced MDSCs, 1.0×10^5 BMP-4–transduced MDSCs, and 2.0×10^5 OA chondrocytes (VEGF/BMP-4–MDSC plus chondrocytes group), 3) 2.0×10^5 BMP-4–transduced MDSCs and 2.0×10^5 OA chondrocytes (BMP-4–MDSC plus chondrocytes group), 4) 2.0×10^5 nontransduced MDSCs and 2.0×10^5 OA chondrocytes (MDSC plus chondrocytes group), and 5) 2.0×10^5 OA chondrocytes (chondrocytes group). Pellets were made in 0.5 ml of chondrogenic medium. The pellets were incubated at 37°C in 5% CO_2, and the medium was changed every 2–3 days. Pellets were harvested after 14 days in culture.

ELISA assessment of VEGF levels. VEGF levels in the medium were measured 48 hours after pellet culture in both mixed pellet culture and pellet coculture using an ELISA kit according to the recommendations of the manufacturer (R&D Systems) (n = 3 in each group).

Alcian blue staining. Paraffin sections of the pellets were deparaffinized, placed in 3% acetic acid for 3 minutes, and transferred into Alcian blue solution (pH 2.5) for 30 minutes. The slides were rinsed with running tap water for 10 minutes and counterstained with nuclear fast red.

Differentiation of MDSCs into chondrocytes. Pellets in OCT blocks were sectioned and prepared for staining as described above. To detect mouse cells in the pellets, double immunohistochemistry (n = 3) was performed as described above. To assess the contribution of each MDSC, the number of double-positive cells and Col2-positive cells was determined in 5 randomly selected soft tissue fields in the pellets, and the average value was calculated.

Quantitative real-time reverse transcriptase–polymerase chain reaction (PCR) analysis of pellet cultured cells. Messenger RNA was isolated using the RNeasy Plus kit, according to the recommendations of the manufacturer (Qiagen, Valencia, CA). After RNA extraction, quantitative PCR analysis of pellets was carried out as described previously (32). Gene expression levels were calculated based on the ΔC_t method. All target genes were normalized to the housekeeping gene *18S*; *18S* primers and probes were designed by and purchased from Applied Biosystems (Foster City, CA). Primers and probes were designed for Col2, SOX9, and type X collagen (Col10) according to GenBank sequence. All target gene primers and probes were purchased from Integrated DNA Technologies (Coralville, IA). For quantitative PCR assays, the coefficients of variation calculated from triplicate assays were within 3%.

The following primer sequences and probes were used: for mouse Col2, forward AAG-TCA-CTG-AAC-AAC-CAG-ATT-GAG-A, reverse AAG-TGC-GAG-CAG-GGT-TCT-TG, and TaqMan probe ATC-CGC-AGC-CCC-GAC-GGC-T; for mouse SOX9, forward CGG-CTC-CAG-CAA-GAA-CAA-G, reverse TGC-GCC-CAC-ACC-ATG-A, and TaqMan probe ACG-TCA-AGC-GAC-CCA-TGA-ACG-C; and for mouse Col10, forward TAC-TTA-CAC-GGA-TGG-AGA-CCA-TGT-T, reverse ATC-CAG-TTG-ACT-ACT-GGT-GCA-ATT-T, and TaqMan probe AAC-CCT-CTT-TTC-GGA-TTA-ACC-CTG-CGA-GTT.

Fluorescence in situ hybridization (FISH). Slides from frozen sections were fixed with 4% paraformaldehyde, air dried, and then dehydrated in a series of successive concentrations of 70%, 80%, 95%, and 100% ethanol for 3 minutes each. Slides were incubated in pepsin solution for 5 minutes, then washed in 2× sodium chloride–sodium citrate (SSC), and dehydrated. FITC-conjugated mouse Y chromosome probe and rhodamine-conjugated rat X chromosome were mixed with hybridization buffer according to the recommendations of the manufacturer (IDLabs Biotechnology, London, Ontario, Canada) and were applied to the target area on the slide, covered with a coverslip, and sealed with rubber cement. After the cement had dried (~10 minutes at room temperature), the slides and probe were codenatured by placing on a heating block (Fisher, Kalamazoo, MI) set at 68.5°C for 5 minutes followed by hybridization overnight in a prewarmed, opaque humidified chamber at 37°C. On day 2, the rubber cement and coverslips were removed by soaking briefly in 2× SSC solution (pH 7.0) at 45°C. Excess probe was rinsed with 50% formamide–2× SSC for 12 minutes; followed by 20 minutes in 2× SSC at 45°C. Nuclei were counterstained with DAPI.

Statistical analysis. All values are expressed as the mean ± SEM. Paired *t*-tests were performed for comparison of data before and after treatment. The comparisons among the 5 groups were made using one-way analysis of variance. Post hoc analysis was performed using Fisher's protected least significant difference test. Histologic scores were compared using the Kruskal-Wallis test. *P* values less than 0.05 were considered significant.

RESULTS

Macroscopic and histologic findings in the joints. Transduced MDSCs were injected into the joint capsule 2 weeks after MIA injection (n = 30 rats [60 OA knees]). The animals were divided into 5 treatment groups (sFlt-1/BMP-4–MDSC, VEGF/BMP-4–MDSC, BMP-4–MDSC, nontransduced MDSC, and PBS groups). MDSCs used were retrovirally transduced with GFP, BMP-4–GFP, sFlt-1–LacZ, or VEGF-LacZ. There was no gross evidence of any side effects such as infection or tumor formation throughout the observation period.

Four weeks after MDSC transplantation into the OA model (2 weeks of induction), macroscopic evaluation of the sFlt-1/BMP-4–transduced MDSC group re-

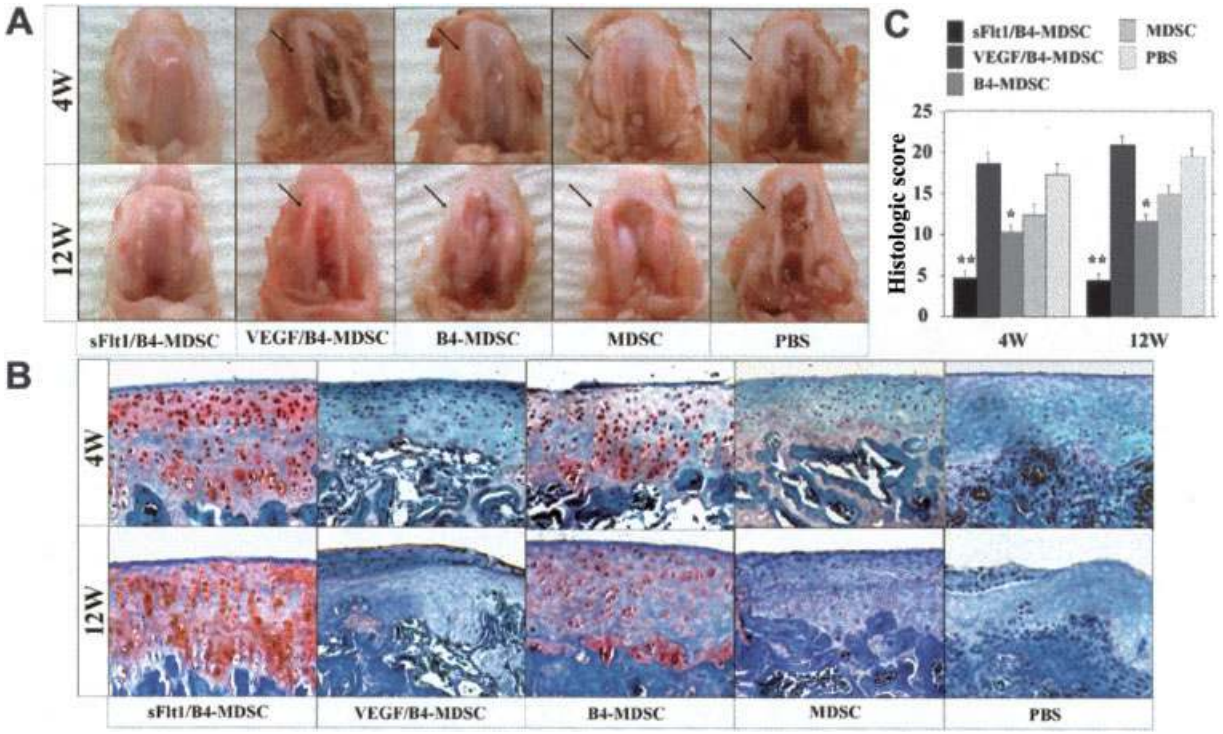

Figure 1. **A** and **B**, Macroscopic (**A**) and histologic (**B**) evaluation of representative joints from rats injected with muscle-derived stem cells (MDSCs) transduced with soluble Flt-1 (sFlt-1) and bone morphogenetic protein 4 (BMP-4 [B4]) (sFlt-1/BMP-4–MDSC), MDSCs transduced with vascular endothelial growth factor (VEGF) and BMP-4 (VEGF/BMP-4–MDSC), MDSCs transduced with BMP-4 alone (BMP-4–MDSC), nontransduced MDSCs (MDSC), or phosphate buffered saline (PBS) alone, 4 and 12 weeks after transplantation. Four weeks after transplantation, the sFlt-1/BMP-4–MDSC and BMP-4–MDSC groups macroscopically and histologically showed smooth joint surface with well-repaired articular cartilage and Safranin O–positive hyaline-like cartilage (red staining in **B**). However, the other groups showed marked arthritic progression, synovial hypertrophy, and osteophyte formation (**arrows**). Twelve weeks after transplantation, although the sFlt-1/BMP-4–MDSC group still showed well-repaired articular cartilage, the other groups exhibited more severe arthritis compared with 4 weeks. (Original magnification × 100.) **C**, Semiquantitative histologic scores for all groups, 4 and 12 weeks following transplantation. The sFlt-1/BMP-4–MDSC group had the lowest (best) scores of all groups. Bars show the mean and SEM. ** = $P < 0.05$ versus all other groups; * = $P < 0.05$ versus the VEGF/BMP-4–MDSC, MDSC, and PBS groups.

vealed smooth joint surfaces of articular cartilage and no osteophyte formation (Figure 1A). Although the BMP-4–transduced MDSC group also showed well-healed articular surfaces, some parts of the joints included osteophyte formation (Figure 1A). However, the VEGF/BMP-4–MDSC, nontransduced MDSC, and PBS groups showed marked arthritis including synovial hypertrophy and osteophyte formation (Figure 1A).

Histologic assessment demonstrated that Safranin O–positive hyaline-like cartilage was present in the sFlt-1/BMP-4–MDSC and BMP-4–MDSC groups only, and the BMP-4—MDSC group had much less Safranin O staining than did the sFlt-1/BMP-4–MDSC group (Figure 1B). However, Safranin O–positive hyaline-like cartilage was less prominent in the nontransduced MDSC group and was completely absent in both the VEGF/BMP-4–MDSC and PBS groups (Figure 1B).

Twelve weeks after transplantation, rat knees treated with sFlt-1/BMP-4–MDSCs still showed smooth joint surfaces in most regions of the articular condyles (Figure 1A). In the BMP-4–MDSC group, although the articular cartilage surfaces tended to be smooth, osteophyte formation was more advanced than at 4 weeks (Figure 1A). The VEGF/BMP-4–MDSC, nontransduced MDSC, and PBS groups showed marked progression of arthritis (Figure 1A). Histologic assessment also demonstrated that more Safranin O–positive tissue and fewer clusters of chondrocytes near necrotic tissue were found in the sFlt-1/BMP-4–MDSC and BMP-4–MDSC groups compared with the other groups (Figure 1B). Destructive events, including pannus invasion, osteolysis, cyst formation within the subchondral bone area, and cartilage tissue lacking Safranin O–positive staining were observed in the VEGF/BMP-4–MDSC and PBS groups (Figure 1B).

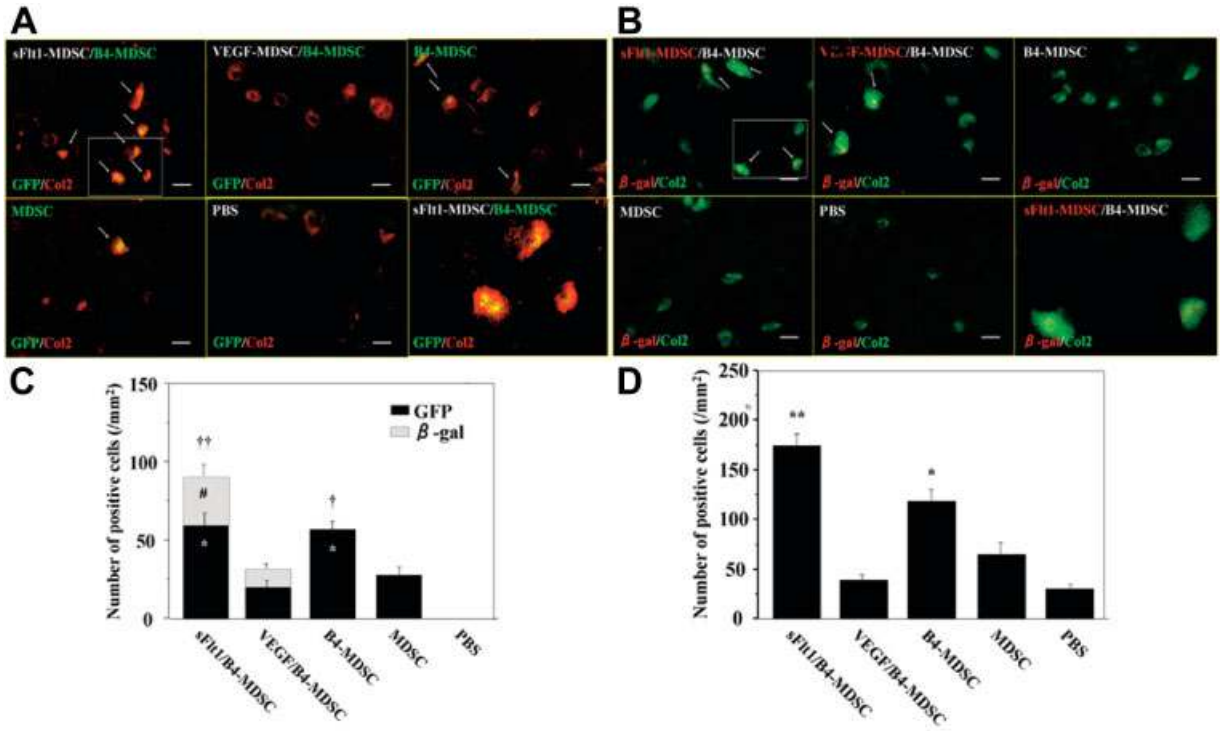

Figure 2. Contribution of MDSCs to cartilage regeneration and repair. **A,** Double immunohistochemical staining for type II collagen (Col2) and green fluorescent protein (GFP). The sFlt-1/BMP-4–MDSC and BMP-4–MDSC groups showed significantly higher levels of chondrogenic differentiation than did the other groups. **B,** Double immunohistochemical staining for Col2 and β-galactosidase (β-gal). The sFlt-1/BMP-4–MDSC group showed higher levels of chondrogenic differentiation than did the VEGF/BMP-4–MDSC group. In **A** and **B,** the last panel shows a higher-magnification view of the boxed area in the first panel. **Arrows** show double-positive cells. Bars = 20 μm. **C,** Numbers of GFP-positive and β-gal–positive cells in each group. The total chondrogenic differentiation of MDSCs was significantly greater in the sFlt-1/BMP-4–MDSC group than in the other groups. Bars show the mean and SEM. $*$ = $P < 0.05$ versus the VEGF/BMP-4–MDSC and MDSC groups; †† = $P < 0.05$ versus all other groups; † = $P < 0.05$ versus the VEGF/BMP-4–MDSC, MDSC, and PBS groups; # = $P < 0.05$ versus the VEGF/BMP-4–MDSC group. **D,** Total number of Col2-positive cells in each group. The sFlt-1/BMP-4–MDSC group had a significantly greater number of chondrocytes than did the other groups. Bars show the mean and SEM. $**$ = $P < 0.05$ versus all other groups; $*$ = $P < 0.05$ versus the VEGF/BMP-4–MDSC, MDSC, and PBS groups. See Figure 1 for other definitions.

A previously described histologic grading scale (28) was used to evaluate the quality of the repaired tissue. Four weeks after transplantation, the total score in the sFlt-1/BMP-4–MDSC group was significantly lower than that in all of the other groups. The score in the BMP-4–MDSC group was significantly lower than the scores in the VEGF/BMP-4–MDSC, nontransduced MDSC, and PBS groups (mean ± SEM score 4.7 ± 0.8 in sFlt-1/BMP-4–MDSC, 18.7 ± 1.3 in VEGF/BMP-4–MDSC, 10.0 ± 1.3 in BMP-4–MDSC, 12.3 ± 1.3 in nontransduced MDSC, and 17.3 ± 0.8 in the PBS group) ($P < 0.01$ for sFlt-1/BMP-4–MDSC versus VEGF/BMP-4–MDSC, nontransduced MDSC, and PBS groups, and for BMP-4–MDSC versus VEGF/BMP-4–MDSC and PBS groups; $P < 0.05$ for sFlt-1/BMP-4–MDSC versus BMP-4–MDSC group, and for BMP-4–MDSC versus nontransduced MDSC group) (Figure 1C).

Twelve weeks after transplantation, the total score in the sFlt-1/BMP-4–MDSC group was also significantly lower than that in all other groups. The score in the BMP-4–MDSC group was significantly lower than the scores in the VEGF/BMP-4–MDSC, nontransduced MDSC, and PBS groups (mean ± SEM score 4.3 ± 0.8 in sFlt-1/BMP-4–MDSC, 20.7 ± 1.3 in VEGF/BMP-4–MDSC, 11.5 ± 0.5 in BMP-4–MDSC, 14.7 ± 0.8 in nontransduced MDSC, and 19.3 ± 1.3 in the PBS group) ($P < 0.01$ for sFlt-1/BMP-4–MDSC versus VEGF/BMP-4–MDSC, nontransduced MDSC, and PBS groups, and for BMP-4–MDSC versus VEGF/BMP-4–MDSC and PBS groups; $P < 0.05$ for sFlt-1/BMP-4–MDSC versus BMP-4–MDSC group, and for BMP-4–MDSC versus nontransduced MDSC group) (Figure 1C). Notably, although the scores in the sFlt-1/BMP-4–MDSC group at 12 weeks were similar to the scores at the 4-week time

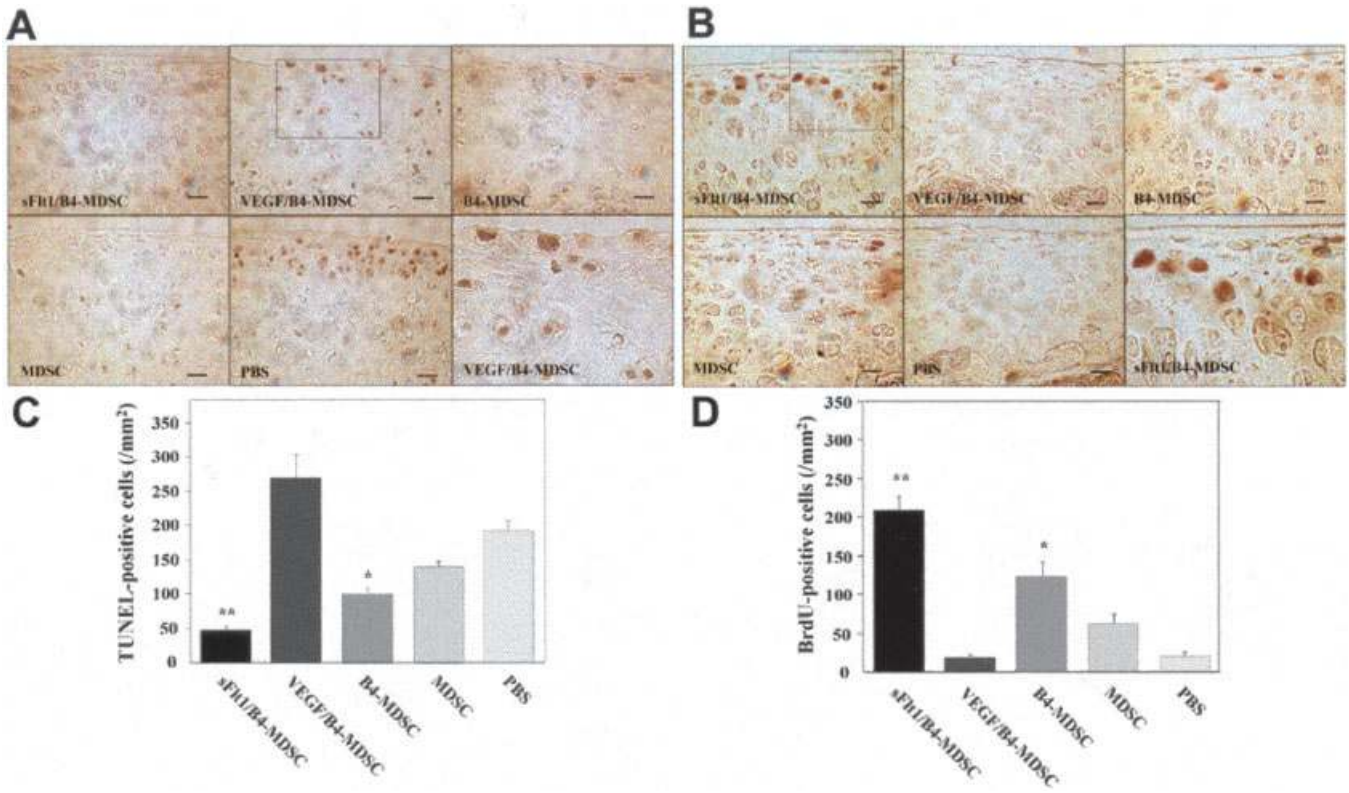

Figure 3. Chondrocyte apoptosis and proliferation. **A,** TUNEL staining in all groups 4 weeks after transplantation. The sFlt-1/BMP-4–MDSC group had significantly fewer apoptotic cells, and the VEGF/BMP-4–MDSC group had a greater number of apoptotic cells, compared with the other groups. **B,** Bromodeoxyuridine (BrdU) assay in all groups 4 weeks after transplantation. The sFlt-1/BMP-4–MDSC group had a significantly greater number of proliferative cells, and the VEGF/BMP-4–MDSC group had fewer proliferative cells, compared with the other groups. In **A** and **B,** the last panel shows a higher-magnification view of the boxed area in the first panel. Bars = 50 μm. **C,** Number of TUNEL-positive cells in each group. **D,** Number of BrdU-positive cells in each group. Bars in **C** and **D** show the mean and SEM. ** = $P < 0.05$ versus all other groups; * = $P < 0.05$ versus the VEGF/BMP-4–MDSC, MDSC, and PBS groups. See Figure 1 for other definitions.

point, all other treatment groups showed variable levels of disease progression.

Contribution of MDSCs to cartilage regeneration and repair. To histologically assess the contribution of the different types of transduced MDSCs to OA healing in these models, double immunohistochemical staining for Col2 and GFP or β-gal was performed using tissue samples obtained 4 weeks after cell injection. Differentiated chondrocytes derived from transduced MDSCs were detected in the superficial and mid-zones of the articular cartilage of the femoral condyle, by double-positive staining for Col2 and either GFP or β-gal, depending on the cell type used. All cells that were transduced to express BMP-4 were also transduced to express GFP. Also, the control MDSCs used for the MDSC group were transduced to express GFP. GFP-positive cells expressing Col2 were found in the femoral condyles in all groups except the PBS control group, which received no GFP-labeled MDSCs (Figure 2A). Cells that were transduced to express VEGF or sFlt-1 were also transduced to express β-gal using the LacZ gene. Within the knee, cells that coexpressed Col2 and β-gal were identified (Figure 2B).

Quantification of the number of cells that were double positive for Col2 and GFP demonstrated that the sFlt-1/BMP-4–MDSC and BMP-4–MDSC groups showed significantly higher numbers of GFP-labeled cells differentiated into Col2-expressing cells (chondrocytes) compared with the VEGF/BMP-4–MDSC and nontransduced MDSC groups (mean ± SEM cells/mm^2 58.7 ± 7.9 in sFlt-1/BMP-4–MDSC, 18.7 ± 4.9 in VEGF/BMP-4–MDSC, 56.0 ± 5.5 in BMP-4–MDSC, and 26.7 ± 5.3 in MDSC) ($P < 0.01$ for sFlt-1/BMP-4–MDSC and BMP-4–MDSC groups versus VEGF/BMP-4–MDSC and nontransduced MDSC groups) (Figure 2C).

Colocalization of Col2 and β-gal demonstrated that the sFlt-1/BMP-4–MDSC group had significantly more β-gal–positive chondrocytes than did the VEGF/BMP-4–MDSC group (mean ± SEM cells/mm^2 29.3 ± 6.4 in sFlt-1/BMP-4–MDSC and 10.7 ± 3.4 in VEGF/

BMP-4–MDSC) ($P < 0.01$) (Figure 2C). Total counts of cells that were double positive for Col2 and either GFP or β-gal indicated that the sFlt-1/BMP-4–MDSC group contained significantly more double-positive cells than did the BMP-4–MDSC, VEGF/BMP-4–MDSC, and nontransduced MDSC groups (mean ± SEM cells/mm^2 88.0 ± 3.6 in sFlt-1/BMP-4–MDSC, 29.3 ± 4.9 in VEGF/BMP-4–MDSC, 56.0 ± 5.5 in BMP-4–MDSC, and 26.7 ± 5.3 in nontransduced MDSC) ($P < 0.01$ for sFlt-1/BMP-4–MDSC versus BMP-4–MDSC, VEGF/BMP-4–MDSC, and MDSC groups, and for BMP-4–MDSC versus VEGF/BMP-4–MDSC and MDSC groups) (Figure 2C).

The total number of Col2-positive cells (chondrocytes from MDSCs and host chondrocytes) was also significantly higher in the sFlt-1/BMP-4–MDSC group than in the other groups (mean ± SEM cells/mm^2 173.3 ± 12.0 in sFlt-1/BMP-4–MDSC, 37.3 ± 3.4 in VEGF/BMP-4–MDSC, 117.3 ± 8.9 in BMP-4–MDSC, 64.0 ± 8.3 in MDSC, and 29.3 ± 2.7 in the PBS group) ($P < 0.01$ for sFlt-1/BMP-4–MDSC versus all other groups; $P < 0.05$ for BMP-4–MDSC versus VEGF/BMP-4–MDSC, MDSC, and PBS groups) (Figure 2D).

Results of chondrocyte apoptosis and proliferation analyses. To analyze chondrocyte apoptosis histologically, TUNEL staining was performed using tissue samples obtained 4 weeks after cell infusion. Chondrocyte apoptosis was less abundant in the superficial and mid-zones of the articular cartilage of the femoral condyle, especially in the sFlt-1/BMP-4–MDSC and BMP-4–MDSC groups compared with the VEGF/BMP-4–MDSC group (Figure 3A). Quantification of TUNEL staining showed that the sFlt-1/BMP-4–MDSC group had significantly fewer apoptotic chondrocytes compared with other treatment groups (mean ± SEM cells/mm^2 46.5 ± 7.1 in sFlt-1/BMP-4–MDSC, 268.5 ± 30.2 in VEGF/BMP-4–MDSC, 99.0 ± 7.3 in BMP-4–MDSC, 138.0 ± 11.3 in MDSC, and 190.5 ± 15.3 in the PBS group) ($P < 0.01$ for sFlt-1/BMP-4–MDSC versus VEGF/BMP-4–MDSC, MDSC, and PBS groups, and for BMP-4–MDSC versus VEGF/BMP-4–MDSC and PBS groups; $P < 0.05$ for sFlt-1/BMP-4–MDSC versus BMP-4–MDSC, and for BMP-4–MDSC versus MDSC) (Figure 3C).

A BrdU incorporation assay was performed on tissue samples from 4-week postoperative animals in order to assess cell proliferation in the knee joint. Proliferating cells were identified primarily in the superficial and mid-zones of the femoral articular cartilage, especially in the sFlt-1/BMP-4–MDSC and BMP-4–MDSC groups (Figure 3B). The number of BrdU-positive chondrocytes was significantly higher in the sFlt-1/BMP-4–MDSC group compared with all other groups (mean ± SEM cells/mm^2 207.0 ± 16.1 in sFlt-1/BMP-4–MDSC, 16.2 ± 3.4 in VEGF/BMP-4–MDSC, 122.4 ± 11.9 in BMP-4–MDSC, 61.2 ± 11.5 in MDSC, and 19.8 ± 1.8 in the PBS group) ($P < 0.01$ for sFlt-1/BMP-4–MDSC versus all other groups, and for BMP-4–MDSC versus VEGF/BMP-4–MDSC and PBS groups; $P < 0.05$ for BMP-4–MDSC versus MDSC) (Figure 3D).

Results of mixed pellet culture. To assess the chondrogenic differentiation of MDSCs and their effects on OA chondrocytes, we performed mixed-cell micromass pellet culture (Figure 4A). ELISA for VEGF levels in the control medium of unmixed pellet culture and in mixed pellet culture showed that VEGF action in MDSCs was blocked by sFlt-1 and significantly enhanced by BMP-4 (mean ± SEM pg/ml per 48 hours 426.7 ± 8.8 in sFlt-1/BMP-4–MDSC plus chondrocytes, 872.0 ± 5.7 in VEGF/BMP-4–MDSC plus chondrocytes, 759.2 ± 15.5 in BMP-4–MDSC plus chondrocytes, 724.9 ± 4.0 in MDSC plus chondrocytes, 270.4 ± 14.8 in chondrocytes alone, 524.9 ± 4.0 in MDSC, 84.3 ± 29.1 in sFlt-1–MDSC, 806.2 ± 7.6 in VEGF-MDSC, and 637.6 ± 19.7 in BMP-4–MDSC) ($P < 0.01$ for all paired comparisons except for BMP-4–MDSC plus chondrocytes versus MDSC plus chondrocytes) (Figure 4B).

Pellets formed using BMP-4–MDSCs and OA chondrocytes were significantly larger than the pellets formed with the other cell types. Also, the pellets formed by mixing cells expressing sFlt-1 were larger than the other mixed-cell combinations, with the exception of the BMP-4–MDSC plus chondrocytes group (mean ± SEM mm 1.40 ± 0.05 in sFlt-1/BMP-4–MDSC plus chondrocytes, 1.13 ± 0.05 in VEGF/BMP-4–MDSC plus chondrocytes, 1.62 ± 0.07 in BMP-4–MDSC plus chondrocytes, 1.22 ± 0.09 in MDSC plus chondrocytes, and 0.93 ± 0.06 in chondrocytes alone) ($P < 0.01$ for BMP-4–MDSC plus chondrocytes versus VEGF/BMP-4–MDSC plus chondrocytes, MDSC plus chondrocytes, and chondrocytes alone, and for sFlt-1/BMP-4–MDSC plus chondrocytes versus chondrocytes alone; $P < 0.05$ for BMP-4–MDSC plus chondrocytes versus sFlt-1/BMP-4–MDSC plus chondrocytes, and for sFlt-1/BMP-4–MDSC plus chondrocytes versus VEGF/BMP-4–MDSC plus chondrocytes and MDSC plus chondrocytes) (Figure 4C).

All of the pellets from every group showed hyaline cartilage–like ECM that stained positively for Alcian blue and contained well-differentiated, round chondrocyte-like cells (Figure 4D). Double immunohistochemical staining for Col2 and either GFP or β-gal showed that chondrocyte-like cells within the pellets

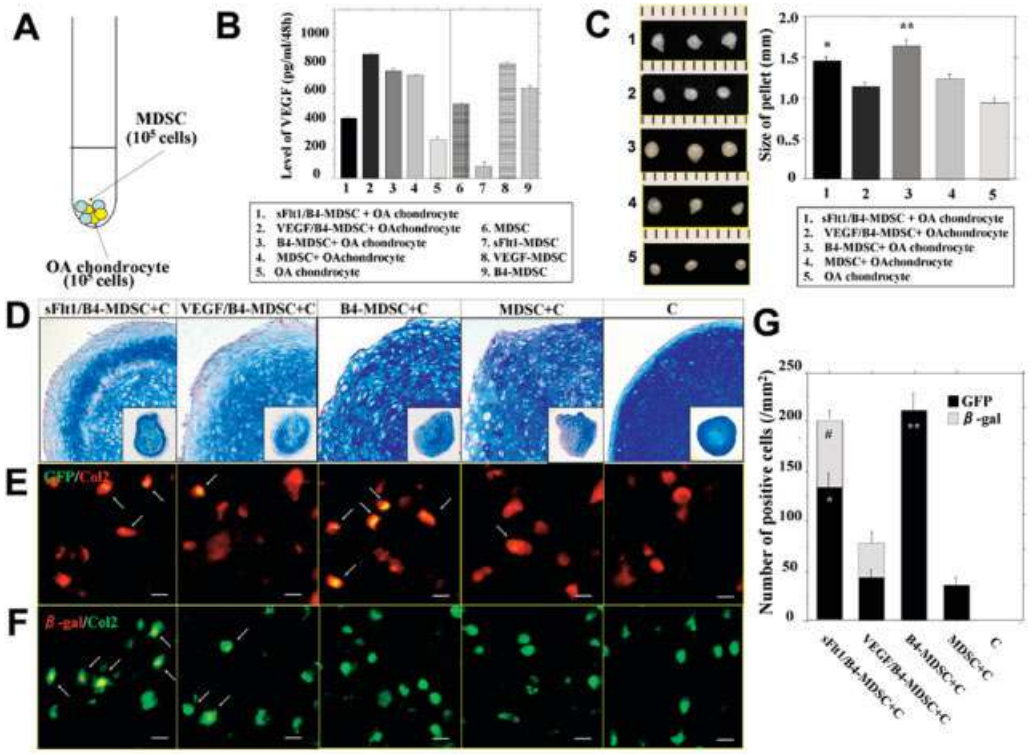

Figure 4. A, Mixed pellet coculture of MDSCs and osteoarthritic (OA) chondrocytes. **B,** Levels of VEGF in the medium of mixed pellet coculture in each group. VEGF activity in MDSCs was blocked by sFlt-1 and enhanced by BMP-4. Bars show the mean and SEM. **C,** Size of pellets in mixed pellet coculture in each group. The BMP-4–MDSC plus chondrocytes group formed significantly larger pellets compared with the other groups. Bars show the mean and SEM. $* = P < 0.05$ versus the VEGF/BMP-4–MDSC plus chondrocytes and MDSC plus chondrocytes groups; $** = P < 0.05$ versus all other groups. **D,** Alcian blue staining in each group. C = OA chondrocytes. **E,** Double immunohistochemical staining for type II collagen (Col2) and green fluorescent protein (GFP). The BMP-4–MDSC plus chondrocytes group formed a significantly greater number of chondrocytes than did the sFlt-1/BMP-4–MDSC plus chondrocytes, VEGF/BMP-4–MDSC plus chondrocytes, and MDSC plus chondrocytes groups. **F,** Double immunohistochemical staining for Col2 and β-galactosidase (β-gal). The sFlt-1/BMP-4–MDSC plus chondrocytes group formed a significantly greater number of chondrocytes than did the VEGF/BMP-4–MDSC plus chondrocytes group. **Arrows** show double-positive cells. Bars = 20 μm. **G,** Numbers of GFP-positive and β-gal–positive cells in each group. Bars show the mean and SEM. $** = P < 0.05$ versus all other groups; $*$ and $\# = P < 0.05$ versus the VEGF/BMP-4–MDSC plus chondrocytes and MDSC plus chondrocytes groups. See Figure 1 for other definitions.

were derived from BMP-4/GFP–MDSCs and GFP-MDSCs in the sFlt-1/BMP-4–MDSC plus chondrocytes, VEGF/BMP-4–MDSC plus chondrocytes, BMP-4–MDSC plus chondrocytes, and MDSC plus chondrocytes groups (Figure 4E) and from the sFlt-1/LacZ–MDSCs and VEGF/LacZ–MDSCs in the sFlt-1/BMP-4–MDSC plus chondrocytes and VEGF/BMP-4–MDSC plus chondrocytes groups (Figure 4F).

The number of double-positive cells was significantly higher in the BMP-4–MDSC plus chondrocytes group compared with sFlt-1/BMP-4–MDSC plus chondrocytes, VEGF/BMP-4–MDSC plus chondrocytes, and MDSC plus chondrocytes groups (mean ± SEM 133.3 ± 16.7 in sFlt-1/BMP-4–MDSC plus chondrocytes, 41.7 ± 8.3 in VEGF/BMP-4–MDSC plus chondrocytes, 208.3 ± 16.7 in BMP-4–MDSC plus chondrocytes, 33.3 ± 8.3 in MDSC plus chondrocytes) ($P < 0.01$ for BMP-4–MDSC plus chondrocytes versus all other groups; sFlt-1/BMP-4–MDSC versus VEGF/BMP-4–MDSC and MDSC groups) (Figure 4G).

Double staining for Col2 and β-gal demonstrated that the number of double-positive cells was significantly higher in the sFlt-1/BMP-4–MDSC plus chondrocytes group compared with the VEGF/BMP-4–MDSC plus chondrocytes group (mean ± SEM mm^2 66.7 ± 8.3 in sFlt-1/BMP-4–MDSC plus chondrocytes and 33.3 ± 8.3

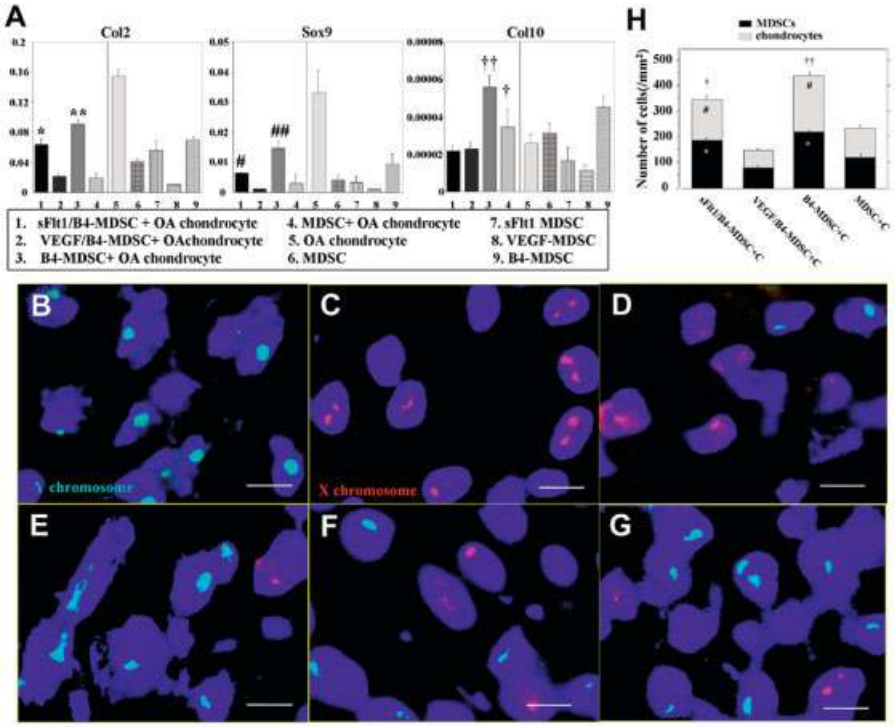

Figure 5. Quantitative polymerase chain reaction (PCR) and fluorescence in situ hybridization (FISH) analysis. **A,** Gene expression of type II collagen (Col2), SOX9, and type X collagen (Col10) in each group, as assessed by quantitative PCR analysis. Pellets from the BMP-4–MDSC plus osteoarthritic (OA) chondrocytes group showed significantly higher gene expression of Col2 and SOX9 than did the other groups; the sFlt-1/BMP-4–MDSC plus chondrocytes group had higher Col2 and SOX9 expression than did the VEGF/BMP-4–MDSC plus chondrocytes and MDSC plus chondrocytes groups. Pellets from the BMP-4–MDSC plus chondrocytes group showed significantly higher gene expression of Col10 than did the other groups; the MDSC plus chondrocytes group had higher Col10 expression than did the sFlt-1/BMP-4–MDSC plus chondrocytes and VEGF/BMP-4–MDSC plus chondrocytes groups. Bars show the mean and SEM. **, ##, and †† = $P < 0.05$ versus all other groups; *, #, and † = $P < 0.05$ versus the sFlt-1/BMP-4–MDSC plus chondrocytes and VEGF/BMP-4–MDSC plus chondrocytes groups. **B–G,** FISH analysis of mixed pellets of normal rat chondrocytes (**B**), mouse MDSCs (**C**), sFlt-1/BMP-4–MDSC plus chondrocytes (**D**), VEGF/BMP-4–MDSC plus chondrocytes (**E**), BMP-4–MDSC plus chondrocytes (**F**), and MDSC plus chondrocytes (**G**), demonstrating that chondrogenic differentiation of mouse MDSCs did not occur through cell fusion (complex of rat X chromosome [red] and mouse Y chromosome [green]). Bars = 20 μm. **H,** Quantification of chondrocytes derived from mouse MDSCs and of rat chondrocytes in each group. The sFlt-1/BMP-4–MDSC plus chondrocytes (C) and BMP-4–MDSC plus chondrocytes groups formed significantly more rat chondrocytes and mouse MDSC–derived chondrocytes than did the other groups. The total number of chondrocytes was significantly higher in the BMP-4–MDSC plus chondrocytes group. Bars show the mean and SEM. * and # = $P < 0.05$ versus the VEGF/BMP-4–MDSC plus chondrocytes and MDSC plus chondrocytes groups; †† = $P < 0.05$ versus all other groups; †= $P < 0.05$ versus the VEGF/BMP-4–MDSC plus chondrocytes and MDSC plus chondrocytes groups. See Figure 1 for other definitions.

in VEGF/BMP-4–MDSC plus chondrocytes) ($P < 0.05$) (Figure 4G).

Quantitative PCR and FISH. Quantitative PCR analysis demonstrated that pellets from the BMP-4–MDSC plus chondrocytes group showed significantly higher gene expression of Col2 than did the sFlt-1/BMP-4–MDSC plus chondrocytes, VEGF/BMP-4–MDSC plus chondrocytes, and MDSC plus chondrocytes groups; Col2 gene expression in the sFlt-1/BMP-4–MDSC plus chondrocytes group was higher than that in the VEGF/BMP-4–MDSC plus chondrocytes and MDSC plus chondrocytes groups (mean ± SEM 0.063 ±

0.0087 in sFlt-1/BMP-4–MDSC plus chondrocytes, 0.022 ± 0.0018 in VEGF/BMP-4–MDSC plus chondrocytes, 0.091 ± 0.0058 in BMP-4–MDSC plus chondrocytes, 0.020 ± 0.0051 in MDSC plus chondrocytes, 0.154 ± 0.0090 in chondrocytes alone, 0.041 ± 0.0020 in MDSC, 0.057 ± 0.012 in sFlt-1–MDSC, 0.011 ± 0.00030 in VEGF-MDSC, and 0.069 ± 0.0043 in BMP-4–MDSC) ($P < 0.01$ for BMP-4–MDSC plus chondrocytes versus sFlt-1/BMP-4–MDSC plus chondrocytes, VEGF/BMP-4–MDSC plus chondrocytes, and MDSC plus chondrocytes, and for sFlt-1/BMP-4–MDSC plus chondrocytes versus VEGF/BMP-4–MDSC plus chondrocytes and MDSC plus chondrocytes) (Figure 5A).

Pellets from the BMP-4–MDSC plus chondrocytes group showed significantly higher gene expression of SOX9 than did those from the sFlt-1/BMP-4–MDSC plus chondrocytes, VEGF/BMP-4–MDSC plus chondrocytes, and MDSC plus chondrocytes groups; SOX9 gene expression was higher in the sFlt-1/BMP-4–MDSC plus chondrocytes group than in the VEGF/BMP-4–MDSC plus chondrocytes and MDSC plus chondrocytes groups (mean ± SEM 0.0064 ± 0.00044 in sFlt-1/BMP-4–MDSC plus chondrocytes, 0.0010 ± 0.00019 in VEGF/BMP-4–MDSC plus chondrocytes, 0.015 ± 0.0021 in BMP-4–MDSC plus chondrocytes, 0.0031 ± 0.0030 in MDSC plus chondrocytes, 0.033 ± 0.0070 in chondrocytes alone, 0.0043 ± 0.0018 in MDSC, 0.0033 ± 0.0021 in sFlt-1–MDSC, 0.0011 ± 0.00014 in VEGF-MDSC, and 0.0092 ± 0.0034 in BMP-4–MDSC) ($P < 0.01$ for BMP-4–MDSC plus chondrocytes versus sFlt-1/BMP-4–MDSC plus chondrocytes, VEGF/BMP-4–MDSC plus chondrocytes, and MDSC plus chondrocytes; $P < 0.01$ for sFlt-1/BMP-4–MDSC plus chondrocytes versus VEGF/BMP-4–MDSC plus chondrocytes and MDSC plus chondrocytes) (Figure 5A).

Additionally, pellets from the BMP-4–MDSC plus chondrocytes group showed significantly higher gene expression of Col10 than did those from the other groups; Col10 gene expression was higher in the MDSC plus chondrocytes group than in the sFlt-1/BMP-4–MDSC plus chondrocytes and VEGF/BMP-4–MDSC plus chondrocytes groups (mean ± SEM 0.000022 ± 0.0000031 in sFlt-1/BMP-4–MDSC plus chondrocytes, 0.000023 ± 0.0000036 in VEGF/BMP-4–MDSC plus chondrocytes, 0.000056 ± 0.0000056 in BMP-4–MDSC plus chondrocytes, 0.000034 ± 0.000011 in MDSC plus chondrocytes, 0.000026 ± 0.0000072 in chondrocytes alone, 0.000031 ± 0.0000049 in MDSC, 0.000016 ± 0.0000072 in sFlt-1–MDSC, 0.000012 ± 0.0000022 in VEGF-MDSC, and 0.000045 ± 0.0000057 in BMP-4–MDSC) ($P < 0.01$ for BMP-4–MDSC plus chondrocytes versus sFlt-1/BMP-4–MDSC plus chondrocytes, VEGF/BMP-4–MDSC plus chondrocytes, and MDSC plus chondrocytes, and for MDSC plus chondrocytes versus sFlt-1/BMP-4–MDSC plus chondrocytes and VEGF/BMP-4–MDSC plus chondrocytes) (Figure 5A).

To determine whether the chondrogenic differentiation of MDSCs occurred through fusion of MDSCs with chondrocytes or through direct differentiation of the MDSCs, we performed FISH with mouse Y chromosomes (from male mouse MDSCs) and rat X chromosomes (from rat OA chondrocytes). The specificity of the probes was tested in pellets of normal rat chondrocytes (Figure 5B) and mouse MDSCs (Figure 5C). The FISH analysis revealed no nuclei in which the mouse Y chromosome colocalized with the rat X chromosome (Figures 5D–G), suggesting that cellular fusion between MDSCs and OA chondrocytes was unlikely in this experiment (Figures 5D–G).

The FISH analysis also demonstrated that the number of MDSCs was significantly higher in the sFlt-1/BMP-4–MDSC plus chondrocytes (Figure 5D) and BMP-4–MDSC plus chondrocytes groups (Figure 5F) than in the VEGF/BMP-4–MDSC plus chondrocytes (Figure 5E) and MDSC plus chondrocytes groups (Figure 5G) (mean ± SEM number/mm^2 182.7 ± 6.8 in sFlt-1/BMP-4–MDSC plus chondrocytes, 78.7 ± 8.7 in VEGF/BMP-4–MDSC plus chondrocytes, 217.3 ± 9.0 in BMP-4–MDSC plus chondrocytes, and 118.0 ± 7.6 in MDSC plus chondrocytes) ($P < 0.01$ for BMP-4–MDSC plus chondrocytes versus all other groups and for sFlt-1/BMP-4–MDSC plus chondrocytes versus VEGF/BMP-4–MDSC plus chondrocytes and MDSC plus chondrocytes groups) (Figure 5H).

Notably, the number of rat chondrocytes was also significantly higher in the sFlt-1/BMP-4–MDSC plus chondrocytes and BMP-4–MDSC plus chondrocytes groups than in the VEGF/BMP-4–MDSC plus chondrocytes and MDSC plus chondrocytes groups (mean ± SEM number/mm^2 158.7 ± 16.7 in sFlt-1/BMP-4–MDSC plus chondrocytes, 66.0 ± 4.2 in VEGF/BMP-4–MDSC plus chondrocytes, 218.0 ± 12.1 in BMP-4–MDSC plus chondrocytes, and 115.3 ± 5.9 in MDSC plus chondrocytes) ($P < 0.01$ for BMP-4–MDSC plus chondrocytes versus all other groups, and for sFlt-1/BMP-4–MDSC plus chondrocytes versus VEGF/BMP-4–MDSC plus chondrocytes and MDSC plus chondrocytes groups) (Figure 5H).

The total number of rat chondrocytes and MDSCs was significantly higher in the BMP-4–MDSC plus chondrocytes group than in all other groups (mean ± SEM number/mm^2 341.3 ± 23.5 in sFlt-1/BMP-4–MDSC plus chondrocytes, 144.7 ± 4.7 in VEGF/BMP-4–MDSC plus chondrocytes, 435.3 ± 19.8

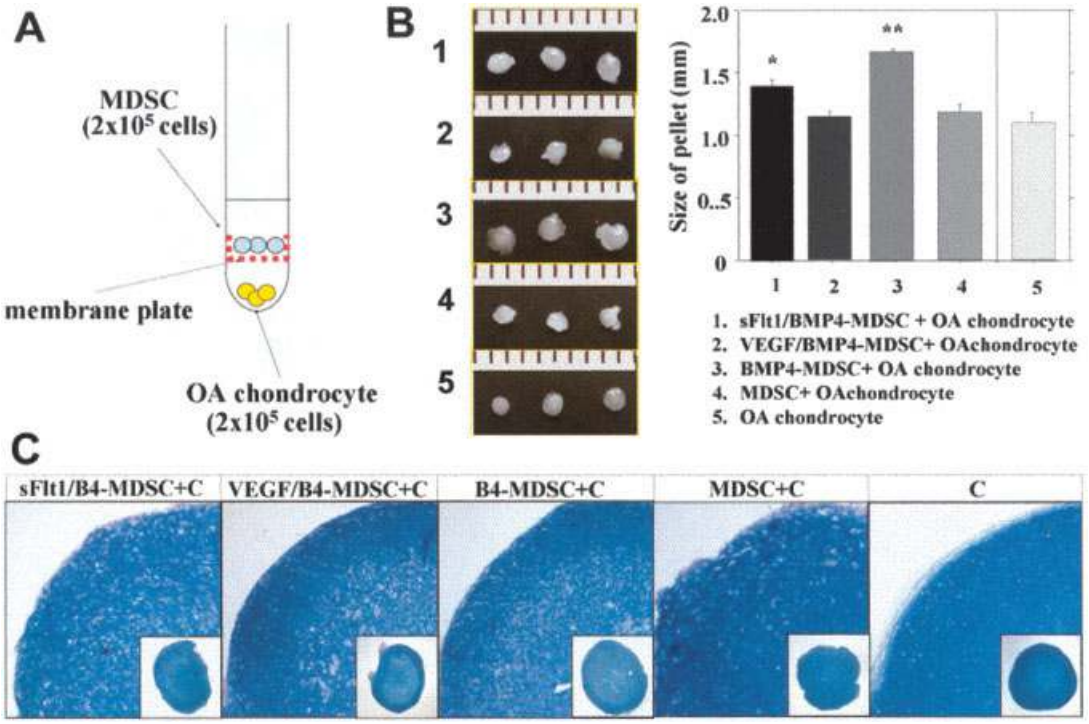

Figure 6. A, Separated pellet coculture of MDSCs and osteoarthritic (OA) chondrocytes. **B,** Size of pellets in each group. OA chondrocytes in the BMP-4–MDSC plus chondrocytes group formed significantly larger pellets compared with the other groups. Bars show the mean and SEM. ** = $P < 0.05$ versus all other groups; * = $P < 0.05$ versus the VEGF/BMP-4–MDSC plus chondrocytes, MDSC plus chondrocytes, and chondrocytes alone groups. **C,** Alcian blue staining in each group. C = OA chrondrocytes (see Figure 1 for other definitions).

in BMP-4–MDSC plus chondrocytes, and 233.3 ± 10.3 in MDSC plus chondrocytes) ($P < 0.01$ for BMP-4–MDSC plus chondrocytes versus all other groups and for sFlt-1/BMP-4–MDSC plus chondrocytes versus VEGF/BMP-4–MDSC plus chondrocytes and MDSC plus chondrocytes groups) (Figure 5H).

Results of separated pellet culture. To assess the chondrogenesis of OA chondrocytes cultured in the presence of factors released by MDSCs, we performed micromass pellet coculture (Figure 6A). Pellet size analysis showed that OA chondrocytes cocultured with BMP-4–MDSCs formed significantly larger pellets compared with all other groups (mean ± SEM mm 1.39 ± 0.04 in sFlt-1/BMP-4–MDSC plus chondrocytes, 1.12 ± 0.07 in VEGF/BMP-4–MDSC plus chondrocytes, 1.65 ± 0.04 in BMP-4–MDSC plus chondrocytes, 1.16 ± 0.03 in MDSC plus chondrocytes, and 1.09 ± 0.07 in chondrocytes alone) ($P < 0.01$ for BMP-4–MDSC plus chondrocytes versus all other groups, and for sFlt-1/BMP-4–MDSC plus chondrocytes versus VEGF/BMP-4–MDSC plus chondrocytes, MDSC plus chondrocytes, and chondrocytes alone) (Figure 6B). All of the pellets from every group showed hyaline cartilage–like ECM that stained positively for Alcian blue and contained well-differentiated, round chondrocytic cells (Figure 6C).

DISCUSSION

Researchers use different rat models of OA to confirm the effectiveness of different treatments. OA-like arthritis is primarily induced by surgical procedures or chemical adjuvants, such as MIA (32–36). Surgically induced OA models may be more clinically relevant than chemically induced models with regard to the pathophysiology of OA. However, there are several drawbacks to surgically induced OA models, including the need for surgical manipulation to induce OA and the difficulty in achieving reproducible levels of severity of arthritis. Therefore, we used an MIA-induced OA model and confirmed the reproducibility of the grade and stage of OA in immunodeficient rats, which was consistent with previous reports of OA in other rat strains (32–34) (Additional information is available upon request from the corresponding author.)

Our in vivo macroscopic and histologic evaluations showed that sFlt-1/BMP-4–transduced MDSCs

had the greatest potential for cartilage repair in the chemically induced OA model. In contrast, the mixture of BMP-4–expressing cells and VEGF-expressing cells led to marked arthritis progression, including synovial hypertrophy, pannus invasion, and osteophyte formation (Figure 1). In a previous study, we found that BMP-4–transduced MDSCs had a higher potential for cartilage regeneration and repair than did nontransduced MDSCs in an osteochondral defect model in the nude rat (13). In the gain- and loss-of-function experiments conducted in the present study, we demonstrated that sFlt-1 improved, and VEGF delayed, cartilage repair with BMP-4–transduced MDSCs in the chemically induced OA model.

Interestingly, in the model of subacute OA the regenerative effects in the sFlt-1/BMP-4–MDSC group were observed up to 16 weeks. (Results in the subacute group are available upon request from the corresponding author.) This same treatment was less effective at the same time in the model in which OA was induced for 2 weeks (chronic OA model). These findings suggest that, to obtain long-term beneficial results, a combined treatment consisting of sFlt-1 (antiangiogenic factor) and BMP-4 with MDSCs is more beneficial in subacute OA than in chronic OA.

In the present study, even when transplanted within the joint space (intraarticularly), MDSCs were found to undergo chondrogenic differentiation, as evidenced by double-positive staining for the GFP or β-gal transgenes and the chondrocyte marker Col2. This showed that both chondrogenic differentiation of transduced MDSCs and intrinsic chondrogenesis were most frequently found in the sFlt-1/BMP-4–treated group, although similar results were found in the BMP-4–transduced MDSC group (Figure 2). In a previous study, we demonstrated that BMP-4 secretion by transduced MDSCs influences the differentiation of multipotent MDSCs toward the chondrogenic lineage in vitro and in vivo (13). Additionally, the present study showed that sFlt-1 improved, while VEGF inhibited, the chondrogenic differentiation of these BMP-4–transduced MDSCs in an OA model.

Furthermore, the intrinsic chondrogenic potential of BMP-4–transduced MDSCs was found to be higher than that of nontransduced MDSCs both in vitro and in vivo. In this study, sFlt-1 enhanced the chondrogenic potential of BMP-4–expressing cells, while VEGF reduced this potential (Figure 2). We reason that the in vivo results that were observed were due to an improvement in chondrogenic differentiation of both the host OA chondrocytes and the implanted MDSCs through the activity of BMP-4, and due to the prevention of vascularization and bone invasion into the regenerated cartilage tissue through the activity of sFlt-1 (23,25).

To attempt to better delineate the mechanism behind the beneficial effects of sFlt-1 and BMP-4 treatment, we performed apoptosis and proliferation assays in vivo (Figure 3). TUNEL assay (apoptosis) results suggested that VEGF induced higher levels of chondrocyte apoptosis and reduced levels of cellular proliferation in the OA knee. In contrast, sFlt-1–treated OA knees showed the lowest level of chondrocyte apoptosis and the highest level of cell proliferation. There are 2 plausible mechanisms by which VEGF may affect cartilage degeneration in OA. VEGF may directly increase catabolic pathways in cartilage tissue through the stimulation of MMP activity and the reduction of TIMPs (23,25). Additionally, VEGF may indirectly cause cartilage destruction by enhancing angiogenesis and vascular invasion, leading to replacement of cartilage by bone. Although the in vivo results presented here support the assertion that VEGF is detrimental to cartilage, we decided to examine whether VEGF worked directly or indirectly on the OA-derived chondrocytes.

In an attempt to establish conditions similar to those in the in vivo experiment, we used in vitro mixed and separated coculture systems to investigate the interaction between transduced MDSCs and OA-derived chondrocytes. The mixed-cell pellet culture showed that, although sFlt-1–transduced and VEGF-transduced MDSCs themselves did not alter chondrogenic potential in an autocrine manner, secreted sFlt-1 enhanced, and VEGF prevented, the chondrogenic differentiation of BMP-4–transduced MDSCs in a paracrine manner. However, BMP-4–transduced MDSCs formed the largest pellets and showed the highest rate of differentiation into chondrocytes (Figure 4). These results indicate that blocking and enhancing VEGF may partially affect the chondrogenic differentiation of BMP-4–transduced MDSCs in vitro, but that BMP-4 itself plays an important role in enhancing the chondrogenic differentiation of MDSCs in an autocrine/paracrine manner, as previously described by our group (13).

In addition, quantitative PCR analysis demonstrated that BMP-4–transduced MDSCs (double dose compared with sFlt-1/BMP-4–MDSCs and VEGF/BMP-4–MDSCs) showed higher gene expression not only of Col2 and SOX9 but also of Col10 (Figure 5A), suggesting that the higher dose of BMP-4 caused differentiation toward hypertrophic chondrocytes. These findings may indicate that a high dose of BMP-4 leads to overproliferation of chondrocytes. In this assay, however, ELISA showed up-regulated VEGF secretion of MDSCs by BMP-4 (Figure 4).

In another previous study, we showed that the beneficial effect of VEGF on bone healing elicited by BMP-4 depended critically on the ratio of VEGF to BMP-4, with an improper ratio leading to detrimental effects on bone healing (26). These findings may indicate that VEGF in moderate concentrations, as opposed to overexpression, maintains chondrocyte survival and control cell differentiation and proliferation in vitro, as previously described (20,37–39). The results of the mixed pellet coculture system indicate that sFlt-1 and BMP-4–expressing MDSCs offer the best balanced combination therapy, despite the fact that the largest pellets in BMP-4–expressing MDSCs also contained the highest gene expression of Col10 (Figures 4 and 5A).

We also tested the separated cell coculture system to investigate the intrinsic effects of sFlt-1, VEGF, and BMP-4 secreted from transduced MDSCs on OA chondrocytes. The results suggest that BMP-4 secreted by MDSCs produced the largest pellets, whereas sFlt-1 enhanced, and VEGF inhibited, the chondrogenic potential of OA chondrocytes to various degrees (Figure 6). These results suggest that BMP-4 mainly affects the redifferentiation or proliferation of OA chondrocytes in vitro. These in vitro mixed and separated pellet coculture experiments suggest the following mechanism: BMP-transduced MDSCs act through an autocrine/paracrine system by releasing BMP-4 that affects the MDSCs themselves, nearby MDSCs, and nearby OA chondrocytes, up-regulating chondrogenesis in vitro. In contrast, VEGF and sFlt-1 secreted by MDSCs have little effect on the chondrogenic differentiation of MDSCs themselves. However, both VEGF and sFlt-1 have some effects on the chondrogenic differentiation of BMP-4–transduced MDSCs and nearby OA chondrocytes.

Stem cells have been reported to undergo multilineage differentiation, but this capacity has recently been a subject of controversy because of possible fusion of stem cells with target-differentiated/lineage-committed cells in the target tissue (39,40). Following these first reports, many researchers reported differentiation of stem cells through fusion with target mature cells, such as hepatocytes with hematopoietic stem cells (41,42), cardiomyocytes with hematopoietic/endothelial progenitor cells (43,44), and neural cells with neural stem cells (45,46). Whether MDSCs undergo chondrogenic differentiation through fusion needed to be addressed.

In addition to characterizing the autocrine/paracrine effect of MDSCs, the present study investigated whether fusion of MDSCs and OA chondrocytes occurred during chondrogenic differentiation. FISH analysis using mixed-cell pellet culture of MDSCs and OA chondrocytes demonstrated no chondrocytes in which the mouse Y chromosome (from the MDSCs) was colocalized with rat X chromosome (from rat OA chondrocytes) (Figures 5B–G), suggesting that there was a lack of fusion between the 2 different cell types. These findings suggest that MDSCs adopted the chondrocyte-like phenotype through potential differentiation without fusion with previously existing chondrocytes. However, the Y chromosome probe is not 100% efficient. This inefficiency may have resulted in an underestimation of the numbers of mouse cells and the possibility that some cell fusion events may have occurred, but were not detected.

In addition, FISH analysis demonstrated the contribution of mouse MDSCs and rat OA chondrocytes. Quantification of the nuclei from cells surrounded by Alcian blue–positive tissue (Figure 4) demonstrated that the total contribution of MDSCs and OA chondrocytes was significantly greater in the BMP-4–MDSC group than in the sFlt-1/BMP-4–MDSC group, consistent with the larger pellet size in the groups that included BMP-4–expressing cells. Taken together, these findings indicate that sFlt-1 may enhance, and VEGF may inhibit, the chondrogenic differentiation of BMP-4–transduced MDSCs and the proliferation of OA chondrocytes; however, these effects are significantly lower than the potential of BMP-4–transduced MDSCs in vitro.

The results of this study support the published data that suggest that VEGF triggers cartilage destruction (23,25,47,48), since we observed that the addition of VEGF inhibited cartilage repair and regeneration or accelerated degeneration in the in vivo OA model. Also, the best histologically assessed regeneration of cartilage in vivo was found in knees treated with both MDSCs expressing BMP-4 and MDSCs expressing sFlt-1, when VEGF signaling was blocked. However, our in vitro results from mixed and separated cell pellet cultures, which were designed to simulate the in vivo situation, showed that the BMP-4–MDSC group had the greatest chondrogenic potential, rather than the sFlt-1/BMP-4–MDSC group. These results suggest that sFlt-1 has more of an enhancing effect in vivo.

With cell markers and flow cytometry, investigators at our laboratory have recently identified and purified a distinct cell population that is developmentally and anatomically related to blood vessels or blood vessel walls within human tissue (49,50). The myoendothelial cells are found in skeletal muscle and coexpress markers of endothelial and myogenic cells (CD34 and CD56) (50). The pericytes are found in multiple human organs including skeletal muscle, pancreas, adipose tis-

sue, and placenta and are isolated based on CD146, nerve/glial antigen 2, and platelet-derived growth factor receptor β expression and absence of hematopoietic, endothelial, and myogenic cell markers (49). These cell populations exhibit multilineage differentiation potential and can, in culture and in vivo, differentiate into myogenic, osteogenic, chondrogenic, and adipogenic cells. In the near future, based on the present findings, we should confirm the potential of this human cell population for cartilage healing and repair in OA.

In conclusion, sFlt-1/BMP-4–transduced MDSCs, VEGF-blocking treatment, which were transplanted intraarticularly in a rat model of OA, enhanced chondrogenesis and chondrogenic regeneration via the autocrine/paracrine effects of BMP-4, and contributed to an appropriate environment that prevented chondrocyte apoptosis by blocking the intrinsic VEGF catabolic pathway and extrinsic VEGF-induced vascular invasion. Blocking VEGF, combined with BMP-4 treatment, of MDSCs is a potentially effective therapy for OA repair that may improve the quality and persistence of regenerated articular cartilage.

ACKNOWLEDGMENTS

The authors are grateful to Jessica Tebbets and Michele Keller for excellent technical help.

AUTHOR CONTRIBUTIONS

Dr. Huard had full access to all of the data in the study and takes responsibility for the integrity of the data and the accuracy of the data analysis.

Study design. Matsumoto, Cooper, Li, Huard.
Acquisition of data. Matsumoto, Gharaibeh, Li, Usas.
Analysis and interpretation of data. Cooper, Gharaibeh, Meszaros, Li, Usas, Fu, Huard.
Manuscript preparation. Matsumoto, Cooper, Gharaibeh, Meszaros, Li, Usas, Fu, Huard.
Statistical analysis. Cooper, Meszaros.
Study oversight and direction. Fu, Huard.

REFERENCES

1. Buckwalter JA, Stanish WD, Rosier RN, Schenck RC Jr, Dennis DA, Coutts RD. The increasing need for nonoperative treatment of patients with osteoarthritis. Clin Orthop Relat Res 2001:36–45.
2. Brittberg M, Lindahl A, Nilsson A, Ohlsson C, Isaksson O, Peterson L. Treatment of deep cartilage defects in the knee with autologous chondrocyte transplantation. N Engl J Med 1994;331: 889–95.
3. Ochi M, Uchio Y, Kawasaki K, Wakitani S, Iwasa J. Transplantation of cartilage-like tissue made by tissue engineering in the treatment of cartilage defects of the knee. J Bone Joint Surg Br 2002;84:571–8.
4. Visna P, Pasa L, Cizmar I, Hart R, Hoch J. Treatment of deep cartilage defects of the knee using autologous chondrograft transplantation and by abrasive techniques—a randomized controlled study. Acta Chir Belg 2004;104:709–14.
5. O'Driscoll SW. The healing and regeneration of articular cartilage. J Bone Joint Surg Am 1998;80:1795–812.
6. Bentley G, Biant LC, Carrington RW, Akmal M, Goldberg A, Williams AM, et al. A prospective, randomised comparison of autologous chondrocyte implantation versus mosaicplasty for osteochondral defects in the knee. J Bone Joint Surg Br 2003;85: 223–30.
7. Qu-Petersen Z, Deasy B, Jankowski R, Ikezawa M, Cummins J, Pruchnic R, et al. Identification of a novel population of muscle stem cells in mice: potential for muscle regeneration. J Cell Biol 2002;157:851–64.
8. Deasy BM, Gharaibeh BM, Pollett JB, Jones MM, Lucas MA, Kanda Y, et al. Long-term self-renewal of postnatal muscle-derived stem cells. Mol Biol Cell 2005;16:3323–33.
9. Oshima H, Payne TR, Urish KL, Sakai T, Ling Y, Gharaibeh B, et al. Differential myocardial infarct repair with muscle stem cells compared to myoblasts. Mol Ther 2005;12:1130–41.
10. Wakitani S, Mitsuoka T, Nakamura N, Toritsuka Y, Nakamura Y, Horibe S. Autologous bone marrow stromal cell transplantation for repair of full-thickness articular cartilage defects in human patellae: two case reports. Cell Transplant 2004;13:595–600.
11. Kuroda R, Ishida K, Matsumoto T, Akisue T, Fujioka H, Mizuno K, et al. Treatment of a full-thickness articular cartilage defect in the femoral condyle of an athlete with autologous bone-marrow stromal cells. Osteoarthritis Cartilage 2007;15:226–31.
12. Adachi N, Sato K, Usas A, Fu FH, Ochi M, Han CW, et al. Muscle derived, cell based ex vivo gene therapy for treatment of full thickness articular cartilage defects. J Rheumatol 2002;29: 1920–30.
13. Kuroda R, Usas A, Kubo S, Corsi K, Peng H, Rose T, et al. Cartilage repair using bone morphogenetic protein 4 and muscle-derived stem cells. Arthritis Rheum 2006;54:433–42.
14. Wakitani S, Goto T, Pineda SJ, Young RG, Mansour JM, Caplan AI, et al. Mesenchymal cell-based repair of large, full-thickness defects of articular cartilage. J Bone Joint Surg Am 1994;76: 579–92.
15. Koga H, Muneta T, Ju YJ, Nagase T, Nimura A, Mochizuki T, et al. Synovial stem cells are regionally specified according to local microenvironments after implantation for cartilage regeneration. Stem Cells 2007;25:689–96.
16. Moses MA, Wiederschain D, Wu I, Fernandez CA, Ghazizadeh V, Lane WS, et al. Troponin I is present in human cartilage and inhibits angiogenesis. Proc Natl Acad Sci U S A 1999;96:2645–50.
17. Shukunami C, Oshima Y, Hiraki Y. Chondromodulin-I and tenomodulin: a new class of tissue-specific angiogenesis inhibitors found in hypovascular connective tissues. Biochem Biophys Res Commun 2005;333:299–307.
18. Robinson CJ, Stringer SE. The splice variants of vascular endothelial growth factor (VEGF) and their receptors. J Cell Sci 2001;114(Pt 5):853–65.
19. Thomas KA. Vascular endothelial growth factor, a potent and selective angiogenic agent. J Biol Chem 1996;271:603–6.
20. Maes C, Stockmans I, Moermans K, van Looveren R, Smets N, Carmeliet P, et al. Soluble VEGF isoforms are essential for establishing epiphyseal vascularization and regulating chondrocyte development and survival. J Clin Invest 2004;113:188–99.
21. Gerber HP, Vu TH, Ryan AM, Kowalski J, Werb Z, Ferrara N. VEGF couples hypertrophic cartilage remodeling, ossification and angiogenesis during endochondral bone formation. Nat Med 1999;5:623–8.
22. Hashimoto S, Creighton-Achermann L, Takahashi K, Amiel D, Coutts RD, Lotz M. Development and regulation of osteophyte formation during experimental osteoarthritis. Osteoarthritis Cartilage 2002;10:180–7.
23. Pufe T, Harde V, Petersen W, Goldring MB, Tillmann B, Mentlein R. Vascular endothelial growth factor (VEGF) induces matrix metalloproteinase expression in immortalized chondrocytes. J Pathol 2004;202:367–74.
24. Pfander D, Kortje D, Zimmermann R, Weseloh G, Kirsch T,

Gesslein M, et al. Vascular endothelial growth factor in articular cartilage of healthy and osteoarthritic human knee joints. Ann Rheum Dis 2001;60:1070–3.
25. Enomoto H, Inoki I, Komiya K, Shiomi T, Ikeda E, Obata K, et al. Vascular endothelial growth factor isoforms and their receptors are expressed in human osteoarthritic cartilage. Am J Pathol 2003;162:171–81.
26. Peng H, Wright V, Usas A, Gearhart B, Shen HC, Cummins J, et al. Synergistic enhancement of bone formation and healing by stem cell-expressed VEGF and bone morphogenetic protein-4. J Clin Invest 2002;110:751–9.
27. Peng H, Chen ST, Wergedal JE, Polo JM, Yee JK, Lau KH, et al. Development of an MFG-based retroviral vector system for secretion of high levels of functionally active human BMP4. Mol Ther 2001;4:95–104.
28. Peng H, Usas A, Olshanski A, Ho AM, Gearhart B, Cooper GM, et al. VEGF improves, whereas sFlt1 inhibits, BMP2-induced bone formation and bone healing through modulation of angiogenesis. J Bone Miner Res 2005;20:2017–27.
29. Pritzker KP, Gay S, Jimenez SA, Ostergaard K, Pelletier JP, Revell PA, et al. Osteoarthritis cartilage histopathology: grading and staging. Osteoarthritis Cartilage 2006;14:13–29.
30. Johnstone B, Hering TM, Caplan AI, Goldberg VM, Yoo JU. In vitro chondrogenesis of bone marrow-derived mesenchymal progenitor cells. Exp Cell Res 1998;238:265–72.
31. Jadlowiec J, Koch H, Zhang X, Campbell PG, Seyedain M, Sfeir C. Phosphophoryn regulates the gene expression and differentiation of NIH3T3, MC3T3-E1, and human mesenchymal stem cells via the integrin/MAPK signaling pathway. J Biol Chem 2004;279: 53323–30.
32. Van der Kraan PM, Vitters EL, van de Putte LB, van den Berg WB. Development of osteoarthritic lesions in mice by "metabolic" and "mechanical" alterations in the knee joints. Am J Pathol 1989;135:1001–14.
33. Guingamp C, Gegout-Pottie P, Philippe L, Terlain B, Netter P, Gillet P. Mono-iodoacetate–induced experimental osteoarthritis: a dose–response study of loss of mobility, morphology, and biochemistry. Arthritis Rheum 1997;40:1670–9.
34. Janusz MJ, Hookfin EB, Heitmeyer SA, Woessner JF, Freemont AJ, Hoyland JA, et al. Moderation of iodoacetate-induced experimental osteoarthritis in rats by matrix metalloproteinase inhibitors. Osteoarthritis Cartilage 2001;9:751–60.
35. Stoop R, Buma P, van der Kraan PM, Hollander AP, Billinghurst RC, Meijers TH, et al. Type II collagen degradation in articular cartilage fibrillation after anterior cruciate ligament transection in rats. Osteoarthritis Cartilage 2001;9:308–15.
36. Janusz MJ, Bendele AM, Brown KK, Taiwo YO, Hsieh L, Heitmeyer SA. Induction of osteoarthritis in the rat by surgical tear of the meniscus: inhibition of joint damage by a matrix metalloproteinase inhibitor. Osteoarthritis Cartilage 2002;10: 785–91.
37. Zelzer E, Mamluk R, Ferrara N, Johnson RS, Schipani E, Olsen BR. VEGFA is necessary for chondrocyte survival during bone development. Development 2004;131:2161–71.
38. Zelzer E, Olsen BR. Multiple roles of vascular endothelial growth factor (VEGF) in skeletal development, growth, and repair. Curr Top Dev Biol 2005;65:169–87.
39. Terada N, Hamazaki T, Oka M, Hoki M, Mastalerz DM, Nakano Y, et al. Bone marrow cells adopt the phenotype of other cells by spontaneous cell fusion. Nature 2002;416:542–5.
40. Ying QL, Nichols J, Evans EP, Smith AG. Changing potency by spontaneous fusion. Nature 2002;416:545–8.
41. Camargo FD, Finegold M, Goodell MA. Hematopoietic myelomonocytic cells are the major source of hepatocyte fusion partners. J Clin Invest 2004;113:1266–70.
42. Willenbring H, Bailey AS, Foster M, Akkari Y, Dorrell C, Olson S, et al. Myelomonocytic cells are sufficient for therapeutic cell fusion in liver. Nat Med 2004;10:744–8.
43. Zhang S, Wang D, Estrov Z, Raj S, Willerson JT, Yeh ET. Both cell fusion and transdifferentiation account for the transformation of human peripheral blood CD34-positive cells into cardiomyocytes in vivo. Circulation 2004;110:3803–7.
44. Nygren JM, Jovinge S, Breitbach M, Sawen P, Roll W, Hescheler J, et al. Bone marrow-derived hematopoietic cells generate cardiomyocytes at a low frequency through cell fusion, but not transdifferentiation. Nat Med 2004;10:494–501.
45. Alvarez-Dolado M, Pardal R, Garcia-Verdugo JM, Fike JR, Lee HO, Pfeffer K, et al. Fusion of bone-marrow-derived cells with Purkinje neurons, cardiomyocytes and hepatocytes. Nature 2003; 425:968–73.
46. Chen KA, Laywell ED, Marshall G, Walton N, Zheng T, Steindler DA. Fusion of neural stem cells in culture. Exp Neurol 2006;198: 129–35.
47. Hashimoto S, Ochs RL, Komiya S, Lotz M. Linkage of chondrocyte apoptosis and cartilage degradation in human osteoarthritis. Arthritis Rheum 1998;41:1632–8.
48. Tanaka E, Aoyama J, Miyauchi M, Takata T, Hanaoka K, Iwabe T, et al. Vascular endothelial growth factor plays an important autocrine/paracrine role in the progression of osteoarthritis. Histochem Cell Biol 2005;123:275–81.
49. Crisan M, Yap S, Casteilla L, Chen CW, Corselli M, Park TS, et al. A perivascular origin for mesenchymal stem cells in multiple human organs. Cell Stem Cell 2008;3:301–13.
50. Zheng B, Cao B, Crisan M, Sun B, Li G, Logar A, et al. Prospective identification of myogenic endothelial cells in human skeletal muscle. Nat Biotechnol 2007;25:1025–34.